



**HAL**  
open science

## Ultrafast strain waves reconstruction from coherent acoustic phonons reflection

Kwan To Lai, Daniel Finkelstein-Shapiro, Arnaud Devos, Pierre-Adrien Mante

► **To cite this version:**

Kwan To Lai, Daniel Finkelstein-Shapiro, Arnaud Devos, Pierre-Adrien Mante. Ultrafast strain waves reconstruction from coherent acoustic phonons reflection. *Applied Physics Letters*, 2021, 119 (9), pp.091106. 10.1063/5.0062570 . hal-03334024

**HAL Id: hal-03334024**

**<https://hal.science/hal-03334024v1>**

Submitted on 3 Sep 2021

**HAL** is a multi-disciplinary open access archive for the deposit and dissemination of scientific research documents, whether they are published or not. The documents may come from teaching and research institutions in France or abroad, or from public or private research centers.

L'archive ouverte pluridisciplinaire **HAL**, est destinée au dépôt et à la diffusion de documents scientifiques de niveau recherche, publiés ou non, émanant des établissements d'enseignement et de recherche français ou étrangers, des laboratoires publics ou privés.

# Ultrafast strain waves reconstruction from coherent acoustic phonons reflection

Cite as: Appl. Phys. Lett. **119**, 091106 (2021); doi: [10.1063/5.0062570](https://doi.org/10.1063/5.0062570)

Submitted: 6 July 2021 · Accepted: 17 August 2021 ·

Published Online: 3 September 2021



View Online



Export Citation



CrossMark

Kwan To Lai,<sup>1</sup>  Daniel Finkelstein-Shapiro,<sup>2</sup>  Arnaud Devos,<sup>3</sup>  and Pierre-Adrien Mante<sup>4,a)</sup> 

## AFFILIATIONS

<sup>1</sup>Department of Applied Physics, The Hong Kong Polytechnic University, Hong Kong

<sup>2</sup>Instituto de Química, Universidad Nacional Autónoma de México, Ciudad de México, Mexico

<sup>3</sup>Institut d'Electronique, de Microélectronique et de Nanotechnologie, Unité Mixte de Recherche, CNRS 8250, Villeneuve d'Ascq Cedex, France

<sup>4</sup>Division of Chemical Physics and NanoLund, Lund University, Lund, Sweden

<sup>a)</sup> Author to whom correspondence should be addressed: [pierre-adrien.mante@chemphys.lu.se](mailto:pierre-adrien.mante@chemphys.lu.se)

## ABSTRACT

Picosecond ultrasonics, which studies laser-induced high-frequency strain waves, is a reliable and versatile method for nondestructive materials' characterization. Strain waves are generated through a light interaction with charges and their subsequent relaxation, and these waves conceal a wealth of information on the material. However, strain waves are detected through their convolution with a sensitivity function, which blurs much of this information. Here, we show that the reflection of strain waves at a free surface leads to the appearance of a Fano resonance in the reflectivity spectrum, accompanied by a drastic increase in the detection bandwidth. We take advantage of this feature to provide a method for the reconstruction of strain waves. We apply it to unambiguously highlight the exact origin of the generation of coherent acoustic phonons in Stranski–Krastanov grown quantum dots, revealing that both the wetting layer and quantum dots are responsible for the generation. Our results will offer the possibility to understand better the interaction of light with charges and their interactions with the lattice.

© 2021 Author(s). All article content, except where otherwise noted, is licensed under a Creative Commons Attribution (CC BY) license (<http://creativecommons.org/licenses/by/4.0/>). <https://doi.org/10.1063/5.0062570>

Ultrafast spectroscopy opens a window into the complex relations between sub-systems out of equilibrium<sup>1,2</sup> and allows tracking energy transfer and dissipation.<sup>3,4</sup> Being able to temporally resolve the interaction among photons, electrons, and other quasi-particles has enabled advanced characterization of materials, which, in turn, have greatly improved device performance.<sup>5</sup> A sub-field of this technique, namely, picosecond ultrasonics,<sup>6,7</sup> is concerned with the temporal evolution of high frequency coherent acoustic phonons (CAPs). Picosecond ultrasonics takes advantage of the nature of acoustic phonons to achieve improved material characterization. For example, the relatively slow speed of sound compared to light allows sub-nanometer thickness measurements.<sup>8</sup> It is also a powerful tool to extract mechanical properties of bulk materials<sup>9,10</sup> and nanostructures.<sup>11,12</sup> Finally, since the generated CAPs are a by-product of charge relaxation, the profile of the strain contains information on carrier dynamics such as the electron-phonon interaction<sup>13</sup> or charge diffusion.<sup>14</sup> However, in picosecond ultrasonics, CAPs are detected through a convolution with a sensitivity function that blurs out details of the strain profile.

The most common detection mechanism of CAPs is through the Brillouin scattering of light,<sup>6,15–17</sup> which depends on the optical properties of the material. The frequency response is centered around the Brillouin frequency, which is ranging from few GHz to few hundreds GHz, depending on material, and the bandwidth of the detection is dictated by the penetration depth of light. Consequently, sharp features of the strain cannot be detected, and a full picture of the generation process and the various associated interactions is out of reach. Other detection mechanisms, such as the quantum confined Stark effect,<sup>18</sup> allow larger bandwidth but require a specific sample structure to be used. To overcome this limitation, researchers have developed dedicated experimental setups based on interferometry that give access to surface displacements.<sup>19</sup> While such a method provides accurate description of the strain with a single experiment, it requires extensive calibration of the setup to ensure a correct ratio of *s*- and *p*-polarized light, needed to cancel photoelastic contributions. Recently, time resolved x-ray diffraction has also been used to reconstruct strain waves,<sup>20,21</sup> as they are sensitive to atomic displacements and offer the

possibility to have a quantitative measurement of the strain amplitude. Nevertheless, the complexity of the equipment, especially to achieve an ultrashort x-ray pulse, is an important hurdle to its widespread use.

In this Letter, we show that during the reflection of CAPs at a free surface, their interaction with light abruptly changes from anti-Stokes to Stokes scattering. The two interactions lead to a discontinuity in the response function of the sample, which is responsible for the appearance of a Fano resonance in the frequency domain and accompanied by a large increase in the bandwidth of the detection process. We take advantage of the large bandwidth to develop a procedure to reconstruct the strain waves. We apply the procedure to the strain generated by InAs quantum dots (QDs) grown by the Stranski–Krastanov method on InP. Our strain reconstruction reveals that both the wetting layer (WL) and the quantum dots are participating in the generation of CAPs, thus answering the debate on the role played by each layer. This experimental method can be carried out with a simple transient reflectance setup and will allow the easy reconstruction of the strain in a wide variety of systems, thus permitting to elucidate the ultrashort dynamics of excited electrons.

In picosecond ultrasonics, a femtosecond laser, the pump, is absorbed by a material, leading to the excitation of carriers (Fig. 1). These carriers yield their excess energy to the lattice, thus increasing its temperature and leading to the generation of a strain. Strain waves can also be generated through the deformation potential mechanism, predominantly in semiconductors.<sup>7</sup> This pulse, or coherent acoustic phonons' wavepackets, then propagates within the sample and is

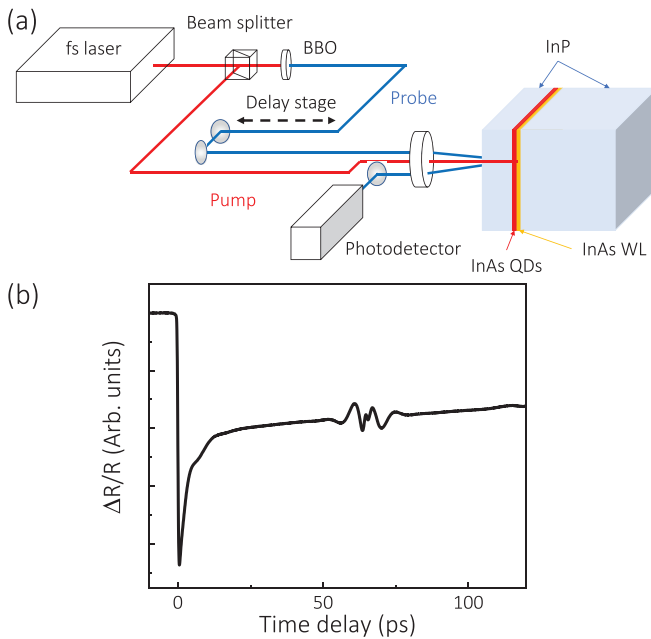


**FIG. 1.** Picosecond ultrasonics. (a) Schematic representation of a picosecond ultrasonic experiment. A femtosecond laser is split into two beams. A first beam is absorbed by the sample and generates coherent acoustic phonons (pump). The second part is time delayed and monitors the evolution of the strain wave (probe). (b) Transient reflectivity measurement obtained on buried InAs quantum dots in InP for a pump wavelength centered at 780 nm and a probe wavelength centered at 390 nm.

reflected at the various interfaces of the material. A second laser pulse, the probe, is time delayed with respect to the pump and detects the temporal evolution of the strain.

Experiments were performed at room temperature on epitaxially grown InAs quantum dots buried in InP.<sup>22,23</sup> The InP orientation is (311), and the thickness of the covering InP layer is 300 nm. The average height of the quantum dots, measured by atomic force microscopy (AFM), is 8 nm,<sup>22,23</sup> and the overall thickness of the phonon-emitting region (quantum dots and the wetting layer) was previously estimated at 12 nm.<sup>24</sup> Photoluminescence experiments show emission of the quantum dots at 1.55  $\mu\text{m}$  and at 1.05  $\mu\text{m}$  for the wetting layer. The time-resolved experiments are carried out using a tunable Ti:sapphire oscillator and a conventional two-color pump and a probe setup at normal incidence. The laser produces 120 fs optical pulses at a repetition rate of 80 MHz, centered at a wavelength tunable between 690 and 1040 nm. In Fig. 1(b), we show the transient reflectivity obtained with a pump wavelength of 780 nm and a probe wavelength of 390 nm, obtained through frequency doubling in a  $\beta$ -barium borate (BBO) crystal. The pump energy is above the bandgap of InP (1.344 eV); however, the penetration depth at this wavelength is sufficient for photons to reach the quantum dots' layer.

At 0 ps, we observe a sharp decay of the reflectivity corresponding to the photoexcitation of carriers by the pump beam. At longer delays, the signal recovers as the carriers yield their excess energy to the lattice and recombine. On top of the signal, we observe a structure at 60 ps. This structure is caused by the reflection at the free surface of the CAPs generated in the QDs region. In the upper part of Fig. 2(a), we zoom in this feature, and we shifted the time axis so that 0 ps corresponds to the center of the reflection, which was determined by considering a successive round trip of the CAPs in the top InP layer. We observe an exponentially growing oscillation corresponding to the strain entering in the penetration depth of the probe. At  $t = 0$  ps, the center of the strain wave is reflected from the free surface and is followed by decaying oscillations corresponding to the CAPs traveling back to the depth of the sample.

The signal, we observe, is a convolution of a sensitivity function,  $f(z)$ , taking into account the optical properties of the material, and the strain,  $\eta(z, t)$ , as depicted in the lower part of Fig. 2(a). In this representation, we consider that the strain is propagating from  $\infty$  to  $-\infty$  and that the interface is located at  $z = 0$ . The transient reflectivity,  $\frac{\Delta R}{R_0}$ , caused by CAPs reflecting at a free surface is given by<sup>17,24</sup>

$$\frac{\Delta R}{R_0} = \int_{-\infty}^{\infty} f(z)\eta(z - vt)dz, \quad (1)$$

where

$$f(z) = \begin{cases} -i\frac{f_0}{2} \left[ \frac{\partial \tilde{n}}{\partial \eta} e^{i\frac{4\pi nz}{\lambda} - \phi} e^{-z/\xi} \right] + c.c., & z > 0, \\ -Ri\frac{f_0}{2} \left[ \frac{\partial \tilde{n}}{\partial \eta} e^{-i\frac{4\pi nz}{\lambda} - \phi} e^{z/\xi} \right] + c.c., & z < 0, \end{cases} \quad (2)$$

with

$$f_0 = 8 \frac{\omega[n^2(n^2 + \kappa^2 - 1)^2 + \kappa^2(n^2 + \kappa^2 + 1)^2]^{1/2}}{c[(n + 1)^2 + \kappa^2]^2} \quad (3)$$

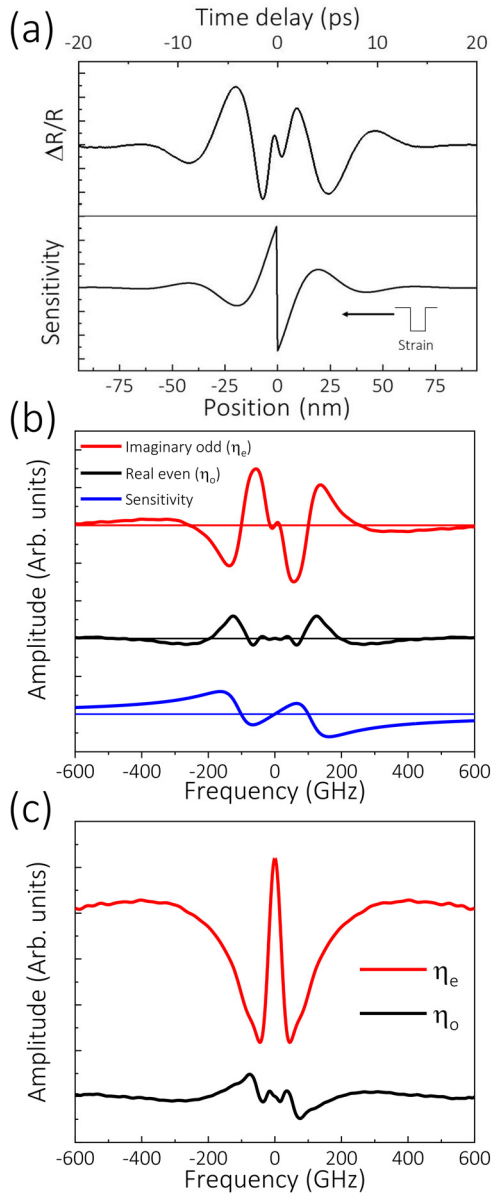


**FIG. 2.** Strain reconstruction procedure. (a) (Upper panel) Transient reflectivity caused by the strain reflection at the free InP surface. (Lower panel) Sensitivity function of InP at 390 nm. The transient reflectivity is the convolution of the strain with the sensitivity function. (b) Real (black) and imaginary (red) part of the Fourier transform of the experimental signal and imaginary part of the Fourier transform of the sensitivity function (blue). (c) Spectra of the even (red) and odd (black) part of the strain obtained by removing the contribution from the sensitivity function.

and

$$\tan \phi = \frac{\kappa(n^2 + \kappa^2 + 1)^2}{n(n^2 + \kappa^2 - 1)^2}. \quad (4)$$

In these expressions,  $v$  is the sound velocity,  $\frac{\partial n}{\partial \eta}$  is the complex photoelastic coefficient,  $\tilde{n} = n + i\kappa$  is the complex refractive index,  $\lambda$

is the probe wavelength,  $R$  is the acoustic reflection coefficient at the free surface, and  $\xi$  is the penetration depth of the probe.

From Eq. (1), we see that the possibility to reconstruct the strain is limited by the bandwidth of the sensitivity function. Equation (2) shows that the response is centered around the Brillouin frequency  $f = 2nv/\lambda$ , and the bandwidth is dictated by the penetration of light. However, we recently demonstrated that during the reflection of an acoustic wave at an interface, the sudden change in momentum of the phonon wave packet leads to a transition from anti-Stokes to Stokes scattering.<sup>17</sup> A consequence of this sudden change is the potential appearance of a discontinuity at  $z=0$  as can be seen in Eq. (2) and in the sensitivity function depicted in Fig. 2(b). This instantaneous change in the sensitivity function will translate into a Fano resonance in the frequency domain accompanied by an extremely large bandwidth, solely limited by the surface roughness of the sample.<sup>17</sup>

The appearance of this extremely high bandwidth offers the possibility to reconstruct the strain, including its high frequency components. Here, we apply the convolution theorem

$$\mathcal{F}\left(\frac{\Delta R}{R_0}\right) = \mathcal{F}(f)\mathcal{F}(\eta). \quad (5)$$

In the following, we will consider that for all frequency components of the strain, the acoustic reflection coefficient is equal to  $-1$ , which is a good approximation given the large acoustic impedance mismatch between InP and air. Furthermore, the surface fluctuations, determined by AFM, in samples like ours are on the order of  $8 \text{ \AA}$ .<sup>23</sup> Using the lowest-order nonlocal small slope approximation,<sup>17,25</sup> we estimate the specular scattering probability to be still larger than 0.96 for frequency as high as 0.6 THz, therefore, justifying the choice of a reflection coefficient equal to  $-1$ .

To facilitate the reconstruction, we take advantage of the parity of the sensitivity function. In Fig. 2(a) and Eq. (2), we see that the sensitivity function is a real, odd function. Consequently, its Fourier transform is imaginary and odd. We now decompose the strain into even,  $\eta_e$ , and odd part,  $\eta_o$ . Their Fourier transforms are real, even and imaginary, odd, respectively. The Fourier transform of the signal, which is a convolution of the strain with the sensitivity function, can, thus, be decomposed into a real, even part, corresponding to  $\eta_o$ , and an imaginary, odd part given by  $\eta_e$ . In Fig. 2(b), we show the real and imaginary part of the Fourier transform of the experimental signal.

The next step for the reconstruction is to remove the contribution from the sensitivity function. We calculated the sensitivity function using Eq. (2) at a wavelength of 390 nm using a refractive index of  $\tilde{n} = 4.0645 + i2.0607$ .<sup>26</sup> We obtain the ratio of photoelastic coefficient by fitting the location of the Fano resonance.<sup>17</sup> From this method, it is not possible to extract the exact value of the photoelastic coefficients, but only their ratio, which in turn does not permit a quantitative determination of the strain amplitude. The resulting sensitivity function is shown in the bottom of Fig. 2(a) and its spectrum in the bottom of Fig. 2(b). This spectrum confirms the large bandwidth that appears as a consequence of the discontinuity during the reflection of the CAPs. We observe that the spectrum is extending beyond 600 GHz and still as an amplitude 10% of its peak amplitude at 2 THz.

By dividing the real and imaginary part of the Fourier transform of the signal by the sensitivity function's spectrum, we obtain the spectra of the strain's even and odd parts, as shown in Fig. 2(c). We observe that the CAPs are predominantly even, which is expected for a

buried generation region, where we expect the strain to be purely dilational or compressive. However, the existence of a non-negligible odd component hints at a complex CAPs emission region, which will be studied in detail in the following.

Finally, the last step in the reconstruction is converting these spectra back to the time domain. We, thus, performed the inverse Fourier transform of the spectra in Fig. 2(c). In Fig. 3(a), we show the temporal shape of  $\eta_e$  and  $\eta_o$ . The complete strain generated by the QD region is then obtained by adding the even and odd contributions and by converting the time into a spatial coordinate by multiplying by the speed of sound in InAs,  $v = 3.83 \text{ nm ps}^{-1}$ .<sup>27</sup>

In Fig. 3(b), we show the reconstructed strain detected for two different experimental conditions with probe (pump) wavelengths of

360 (720) and 390 (780 nm). Since the sensitivity function is dependent on the photoelastic coefficients, the bandwidth of the detection and, thus, the achievable resolution in the reconstruction are highly dependent on the wavelength of the probe. More precisely, the Fano line shape is caused by the interference of a discrete resonance with a continuum of state. In the time domain, this corresponds to the interaction between the resonance at the Brillouin frequency and the discontinuity induced by the transition from anti-Stokes to Stokes scattering, as seen in the lower panel of Fig. 2(a). The sensitivity to high frequency components is due to the sharp transition between anti-Stokes and Stokes scattering and can be enhanced by maximizing the discontinuity. The phase of the oscillations, which dictates the discontinuity, depends on the photoelastic coefficients that are wavelength dependent. Here, we take advantage of the sensitivity of photoelastic coefficients to the electronic structure of the material and tune the wavelength in the vicinity of the  $E_1$  transition to achieve an enhanced detection of high frequency components.<sup>24</sup> The bandwidth for a probe wavelength of 360 nm is much smaller than at 390 nm as shown in the inset of Fig. 3(b). As a consequence, the reconstructed strain is noisier at 360 nm, and features cannot be resolved, contrarily to the strain reconstructed at 390 nm. For a rough surface, diffuse scattering impacts high frequency components much more, which lead to decoherence of the phonon wavepackets, thus reducing the sensitivity to high frequency and the achievable resolution.<sup>17</sup>

The reconstruction method we have developed allows the investigation of the geometric properties of the region of emission. In Fig. 3(b), we can see that the generating region can be divided into two parts with a total thickness of 12 nm, obtained by measuring the FWHM of the strain. This value of 12 nm is in the expected range of the quantum dots' region determined by using cross-sectional transmission electron microscopy.<sup>22</sup> We can also distinguish two regions, where the generation is stronger. We attribute these regions to the quantum dots and the wetting layer. We obtain a wetting layer thickness of 5 nm and an average quantum dot height of 7 nm. Once again, these observations are in good agreement with expected values.<sup>22</sup>

The exact origin of the generation of CAPs in Stranski–Krastanov grown quantum dots has been debated in the past, in particular, the relative contribution of the quantum dots and the wetting layer.<sup>24,28,29</sup> The method we developed allows reconstructing the profile of the strain and unambiguously shows that both regions substantially contribute to the generation of CAPs. In addition to the information provided on the geometry of the generating region, our method could enable retrieving information on the carrier dynamics and, in particular, their diffusion, which impacts the shape of the strain.<sup>14,19</sup>

In conclusion, we developed a procedure to reconstruct the profile of strain generated by the absorption of a femtosecond light pulse. We showed that during the reflection of phonons at a free surface, a discontinuity appears in the interaction of light and sound. This abrupt discontinuity drastically increases the bandwidth of detection and allows complete reconstruction of the generated strain. We use this approach to reconstruct the strain generated by Stranski–Krastanov grown InAs quantum dots on InP. Our reconstruction reveals the significant role played by both the quantum dots and the wetting layer. This reconstruction approach will further enhance the characterization possibilities of picosecond ultrasonics.

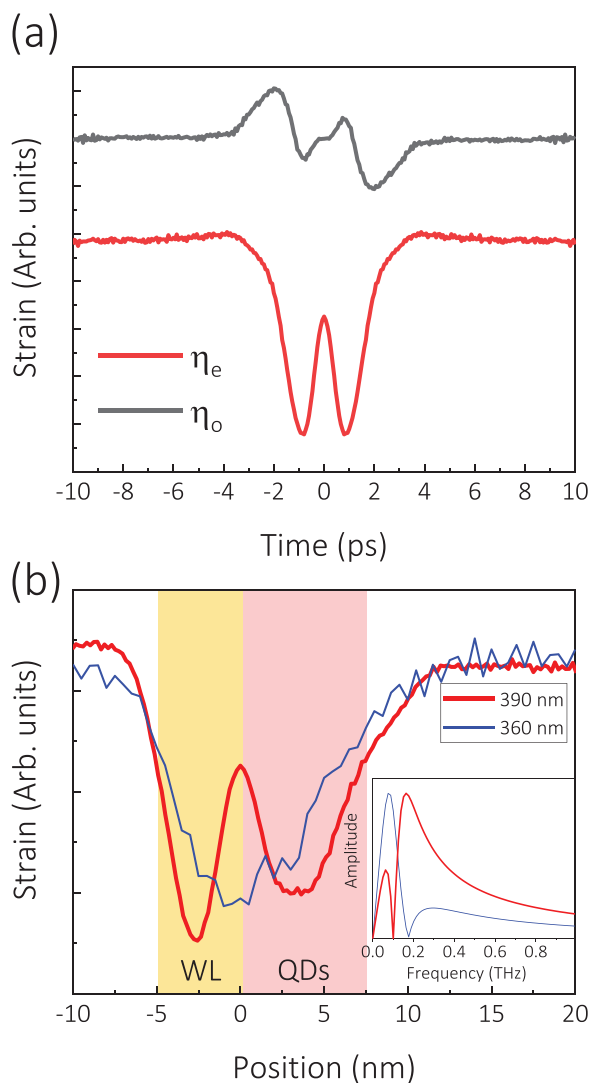


**FIG. 3.** Reconstructed strain generated by quantum dots. (a) Even and odd parts of the strain reconstructed through our procedure. (b) Strain generated by InAs quantum dots grown on InP. We observe a contribution from the quantum dots (QDs) and the wetting layer (WL).

This work was supported by NanoLund, Lunds Universitet, Lund Laser Centre, Crafoordska Stiftelsen, Grant No. 20200630 and Vetenskapsrådet, Grant No. 2017-05150.

## DATA AVAILABILITY

The data that support the findings of this study are available from the corresponding author upon reasonable request.

## REFERENCES

- 1C. Giannetti, M. Capone, D. Fausti, M. Fabrizio, F. Parmigiani, and D. Mihailovic, "Ultrafast optical spectroscopy of strongly correlated materials and high-temperature superconductors: A non-equilibrium approach," *Adv. Phys.* **65**, 58 (2016).
- 2G. M. Müller, J. Walowski, M. Djordjevic, G.-X. Miao, A. Gupta, A. V. Ramos, K. Gehrke, V. Moshnyaga, K. Samwer, J. Schmalhorst, A. Thomas, A. Hütten, G. Reiss, J. S. Moodera, and M. Münzenberg, "Spin polarization in half-metals probed by femtosecond spin excitation," *Nat. Mater.* **8**, 56 (2009).
- 3J.-S. Lauret, C. Voisin, G. Cassabois, C. Delalande, P. Roussignol, O. Jost, and L. Capes, "Ultrafast carrier dynamics in single-wall carbon nanotubes," *Phys. Rev. Lett.* **90**, 057404 (2003).
- 4D. Finkelstein-Shapiro, P.-A. Mante, S. Sarisozen, L. Wittenbecher, I. Minda, S. Balci, T. Pullerits, and D. Zigmantas, "Understanding radiative transitions and relaxation pathways in plexcitons," *Chem* **7**, 1092 (2021).
- 5C. S. Ponseca, T. J. Savenije, M. Abdellah, K. Zheng, A. Yartsev, T. Pascher, T. Harlang, P. Chabera, T. Pullerits, A. Stepanov, J.-P. Wolf, and V. Sundström, "Organometal halide perovskite solar cell materials rationalized: Ultrafast charge generation, high and microsecond-long balanced mobilities, and slow recombination," *J. Am. Chem. Soc.* **136**, 5189 (2014).
- 6C. Thomsen, H. T. Grahn, H. J. Maris, and J. Tauc, "Surface generation and detection of phonons by picosecond light pulses," *Phys. Rev. B* **34**, 4129 (1986).
- 7P. Ruello and V. E. Gusev, "Physical mechanisms of coherent acoustic phonons generation by ultrafast laser action," *Ultrasonics* **56**, 21 (2015).
- 8P.-A. Mante, C.-C. Chen, Y.-C. Wen, H.-Y. Chen, S.-C. Yang, Y.-R. Huang, I. Ju Chen, Y.-W. Chen, V. Gusev, M.-J. Chen, J.-L. Kuo, J.-K. Sheu, and C.-K. Sun, "Probing hydrophilic interface of solid/liquid-water by nanoultrasonics," *Sci. Rep.* **4**, 6249 (2015).
- 9P. Ruello, T. Pezeril, S. Avanesyan, G. Vaudel, V. Gusev, I. C. Infante, and B. Dkhil, "Photoexcitation of gigahertz longitudinal and shear acoustic waves in BiFeO<sub>3</sub> multiferroic single crystal," *Appl. Phys. Lett.* **100**, 212906 (2012).
- 10P.-A. Mante, C. C. Stoumpos, M. G. Kanatzidis, and A. Yartsev, "Directional negative thermal expansion and large Poisson ratio in CH<sub>3</sub>NH<sub>3</sub>PbI<sub>3</sub> perovskite revealed by strong coherent shear phonon generation," *J. Phys. Chem. Lett.* **9**, 3161 (2018).
- 11P. Maioli, T. Stoll, H. E. Saucedo, I. Valencia, A. Demessence, F. Bertorelle, A. Crut, F. Vallée, I. L. Garzón, G. Cerullo, and N. Del Fatti, "Mechanical vibrations of atomically defined metal clusters: From nano- to molecular-size oscillators," *Nano Lett.* **18**, 6842–30247927 (2018).
- 12P.-A. Mante, S. Lehmann, N. Anttu, K. A. Dick, and A. Yartsev, "Nondestructive complete mechanical characterization of zinc blende and wurtzite GaAs nanowires using time-resolved pump-probe spectroscopy," *Nano Lett.* **16**, 4792 (2016).
- 13P.-A. Mante, C. C. Stoumpos, M. G. Kanatzidis, and A. Yartsev, "Electron-acoustic phonon coupling in single crystal CH<sub>3</sub>NH<sub>3</sub>PbI<sub>3</sub> perovskites revealed by coherent acoustic phonons," *Nat. Commun.* **8**, 14398 (2017).
- 14O. B. Wright, B. Perrin, O. Matsuda, and V. E. Gusev, "Ultrafast carrier diffusion in gallium arsenide probed with picosecond acoustic pulses," *Phys. Rev. B* **64**, 081202 (2001).
- 15H. Ogi, T. Shagawa, N. Nakamura, M. Hirao, H. Odaka, and N. Kihara, "Elastic constant and Brillouin oscillations in sputtered vitreous SiO<sub>2</sub> thin films," *Phys. Rev. B* **78**, 134204 (2008).
- 16V. E. Gusev and P. Ruello, "Advances in applications of time-domain Brillouin scattering for nanoscale imaging," *Appl. Phys. Rev.* **5**, 031101 (2018).
- 17K. Lai, D. Finkelstein-Shapiro, S. Lehmann, A. Devos, and P.-A. Mante, "Fano resonance between stokes and anti-stokes Brillouin scattering," *Phys. Rev. Res.* **3**, L032010 (2021).
- 18C.-K. Sun, J.-C. Liang, and X.-Y. Yu, "Coherent acoustic phonon oscillations in semiconductor multiple quantum wells with piezoelectric fields," *Phys. Rev. Lett.* **84**, 179 (2000).
- 19O. Matsuda, M. Tomoda, T. Tachizaki, S. Koiwa, A. Ono, K. Aoki, R. P. Beardsley, and O. B. Wright, "Ultrafast ellipsometric interferometry for direct detection of coherent phonon strain pulse profiles," *J. Opt. Soc. Am. B* **30**, 1911 (2013).
- 20Y. Gao, Z. Chen, Z. Bond, A. Loether, L. E. Howard, S. LeMar, S. White, A. Watts, B. C. Walker, and M. F. DeCamp, "Reconstructing longitudinal strain pulses using time-resolved x-ray diffraction," *Phys. Rev. B* **88**, 014302 (2013).
- 21V. Juvé, R. Gu, S. Gable, T. Maroutian, G. Vaudel, S. Matzen, N. Chigarev, S. Raetz, V. E. Gusev, M. Viret, A. Jarnac, C. Laulhé, A. A. Maznev, B. Dkhil, and P. Ruello, "Ultrafast light-induced shear strain probed by time-resolved x-ray diffraction: Multiferroic BiFeO<sub>3</sub> as a case study," *Phys. Rev. B* **102**, 220303 (2020).
- 22C. Paranthoen, N. Bertru, O. Dehaese, A. Le Corre, S. Loualiche, B. Lambert, and G. Patriarche, "Height dispersion control of InAs/InP quantum dots emitting at 1.55  $\mu\text{m}$ ," *Appl. Phys. Lett.* **78**, 1751 (2001).
- 23C. Paranthoen, C. Platz, G. Moreau, N. Bertru, O. Dehaese, A. Le Corre, P. Miska, J. Even, H. Folliot, C. Labbé, G. Patriarche, J. Simon, and S. Loualiche, "Growth and optical characterizations of InAs quantum dots on InP substrate: Towards a 1.55  $\mu\text{m}$  quantum dot laser," in *Proceedings of the Twelfth International Conference on Molecular Beam Epitaxy [J. Cryst. Growth* **251**, 230 (2003)].
- 24P.-A. Mante, A. Devos, and A. L. Louarn, "Generation of terahertz acoustic waves in semiconductor quantum dots using femtosecond laser pulses," *Phys. Rev. B* **81**, 113305 (2010).
- 25P.-A. Mante, C.-C. Chen, Y.-C. Wen, J.-K. Sheu, and C.-K. Sun, "Thermal boundary resistance between GaN and cubic ice and THz acoustic attenuation spectrum of cubic ice from complex acoustic impedance measurements," *Phys. Rev. Lett.* **111**, 225901 (2013).
- 26D. E. Aspnes and A. A. Studna, "Dielectric functions and optical parameters of Si, Ge, GaP, GaAs, GaSb, InP, InAs, and InSb from 1.5 to 6.0 eV," *Phys. Rev. B* **27**, 985 (1983).
- 27*Semiconductors Group IV Elements and III-V Compounds*, 1st ed., Data in Science and Technology, edited by O. Madelung (Springer Berlin Heidelberg, Berlin, Heidelberg, 1991).
- 28A. Devos, F. Poinsotte, J. Groenen, O. Dehaese, N. Bertru, and A. Ponchet, "Strong generation of coherent acoustic phonons in semiconductor quantum dots," *Phys. Rev. Lett.* **98**, 207402 (2007).
- 29E. Péronne, E. Charron, S. Vincent, S. Sauvage, A. Lemaître, B. Perrin, and B. Jusserand, "Two-color femtosecond strobe lighting of coherent acoustic phonons emitted by quantum dots," *Appl. Phys. Lett.* **102**, 043107 (2013).